

Arteriosclerosis, Thrombosis, and Vascular Biology

JOURNAL OF THE AMERICAN HEART ASSOCIATION

American Heart
Association®



Learn and Live SM

Indirubin-3'-Monoxime Blocks Vascular Smooth Muscle Cell Proliferation by Inhibition of Signal Transducer and Activator of Transcription 3 Signaling and Reduces Neointima Formation In Vivo

Andrea V. Schwaiberger, Elke H. Heiss, Muris Cabaravdic, Tina Oberan, Jan Zaujec, Daniel Schachner, Pavel Uhrin, Atanas G. Atanasov, Johannes M. Breuss, Bernd R. Binder and Verena M. Dirsch

Arterioscler Thromb Vasc Biol 2010;30;2475-2481; originally published online Sep 16, 2010;

DOI: 10.1161/ATVBAHA.110.212654

Arteriosclerosis, Thrombosis, and Vascular Biology is published by the American Heart Association, 7272 Greenville Avenue, Dallas, TX 75214

Copyright © 2010 American Heart Association. All rights reserved. Print ISSN: 1079-5642. Online ISSN: 1524-4636

The online version of this article, along with updated information and services, is located on the World Wide Web at:

<http://atvb.ahajournals.org/cgi/content/full/30/12/2475>

Data Supplement (unedited) at:

<http://atvb.ahajournals.org/cgi/content/full/ATVBAHA.110.212654/DC1>

Subscriptions: Information about subscribing to Arteriosclerosis, Thrombosis, and Vascular Biology is online at

<http://atvb.ahajournals.org/subscriptions/>

Permissions: Permissions & Rights Desk, Lippincott Williams & Wilkins, a division of Wolters Kluwer Health, 351 West Camden Street, Baltimore, MD 21202-2436. Phone: 410-528-4050. Fax: 410-528-8550. E-mail:

journalpermissions@lww.com

Reprints: Information about reprints can be found online at

<http://www.lww.com/reprints>

Indirubin-3'-Monoxime Blocks Vascular Smooth Muscle Cell Proliferation by Inhibition of Signal Transducer and Activator of Transcription 3 Signaling and Reduces Neointima Formation In Vivo

Andrea V. Schwaiberger, Elke H. Heiss, Muris Cabaravdic, Tina Oberan, Jan Zaujec, Daniel Schachner, Pavel Uhrin, Atanas G. Atanasov, Johannes M. Breuss, Bernd R. Binder, Verena M. Dirsch

Objective—Our goal was to examine the influence of indirubin-3'-monoxime (I3MO), a natural product-derived cyclin-dependent kinase inhibitor, on vascular smooth muscle cell (VSMC) proliferation in vitro, experimentally induced neointima formation in vivo, and related cell signaling pathways.

Methods and Results—I3MO dose-dependently inhibited platelet-derived growth factor (PDGF)-BB-induced VSMC proliferation by arresting cells in the G₀/G₁ phase of the cell cycle as assessed by 5-bromo-2'-deoxyuridine incorporation and flow cytometry. PDGF-induced activation of the kinases Akt, Erk1/2, and p38^{MAPK} was not affected. In contrast, I3MO specifically blocked PDGF-, interferon- γ -, and thrombin-induced phosphorylation of signal transducer and activator of transcription 3 (STAT3). Human endothelial cells (EA.hy926) responded to I3MO with increased endothelial nitric oxide synthase activity as assessed via [¹⁴C]L-arginine/[¹⁴C]L-citrulline conversion. The specific STAT3 inhibitor Stattic led to decreased VSMC proliferation, and transient expression of a constitutively active form of STAT3 overcame the I3MO-induced cell cycle arrest in mouse embryonic fibroblasts. In a murine femoral artery cuff model, I3MO prevented neointima formation while reducing STAT3 phosphorylation and the amount of proliferating Ki67-positive cells.

Conclusion—I3MO represses PDGF- and thrombin-induced VSMC proliferation and, in vivo, neointima formation, likely because it specifically blocks STAT3 signaling. This profile and its positive effect on endothelial NO production turns I3MO into a promising lead compound to prevent restenosis. (*Arterioscler Thromb Vasc Biol.* 2010;30:2475-2481.)

Key Words: indirubin ■ vascular smooth muscle cell ■ proliferation ■ neointima ■ STAT3

Restenosis is the major factor hampering the beneficial effect of angioplasty and stenting. Vascular smooth muscle cell (VSMC) proliferation, next to local vascular inflammation, is a critical factor in neointima formation and vascular lumen loss during restenosis. Thus, one current strategy to maintain proper vascular function after angioplasty is to inhibit VSMC proliferation by targeting cell cycle regulation, eg, by drug-eluting stents.^{2,3} Two products, the rapamycin-eluting Cypher stent and the paclitaxel-eluting Taxus stent, were approved by the US Food and Drug Administration in 2003 and 2004, respectively. Although successfully introduced into the market, there are now concerns about an increased risk of late stent thrombosis.⁴ Thus, compounds inhibiting neointima formation with mechanisms differing from those of rapamycin and paclitaxel⁵ may have the potential to be efficient with fewer side effects.

Indirubin, a red isomer of indigo, is the active ingredient of the traditional Chinese medicinal formulation *Danggui Longhui Wan*, used against chronic myelocytic leukemia.⁶ Enzyme-based in vitro studies have indicated that indirubin and its derivatives are potent inhibitors of the cyclin-dependent kinases (CDKs) 1, 2, 4, and 5.⁶⁻⁹ Furthermore, different indirubin derivatives showed antitumor activity in several human cancer cells.^{6,10-14} Moreover, for indirubin-3'-monoxime (I3MO), an in vitro antiinflammatory and anticancer activity had been described on the basis of the inhibition of tumor necrosis factor-induced nuclear factor κ B activation and the subsequent suppression of antiapoptotic and proproliferative gene expression.¹⁴

The aim of this study was to investigate the potential use of I3MO in the prevention of restenosis. We therefore analyzed a possible effect on platelet-derived growth factor (PDGF)-

Received on: January 20, 2009; final version accepted on: September 7, 2010.

From the Department of Pharmacognosy, University of Vienna, A-1090 Vienna, Austria (A.V.S., E.H.H., T.O., D.S., A.G.A., V. M. D.); Department of Vascular Biology and Thrombosis Research, Medical University of Vienna, A-1090 Vienna, Austria (M.C., J.Z., P.U., J.M.B., B.R.B.). Dr Binder died on August 28, 2010. Dr Schwaiberger and Dr Heiss contributed equally to this work.

Correspondence to Verena M. Dirsch, PhD, Department of Pharmacognosy, University of Vienna, Althanstr. 14, A-1090 Vienna, Austria. E-mail verena.dirsch@univie.ac.at

© 2010 American Heart Association, Inc.

Arterioscler Thromb Vasc Biol is available at <http://atvb.ahajournals.org>

DOI: 10.1161/ATVBAHA.110.212654

BB-stimulated VSMC proliferation and endothelial cell function in vitro and examined the influence of I3MO on neointima formation in vivo. We then focused on the signaling pathways that are affected by I3MO.

Methods

An expanded Methods section can be found in the Supplemental Data, available online at <http://atvb.ahajournals.org>.

Cell Culture

VSMCs were isolated from male Sprague-Dawley rat thoracic aortas by enzymatic digestion and cultured as described.¹⁵ The human endothelial cell line EA.hy 926 (kindly provided by Dr C.-J. Edgell, University of North Carolina, Chapel Hill, NC) was cultivated as described by Leikert et al.¹⁶ Mouse embryonic fibroblasts (MEFs) were grown in DMEM supplemented with 10% FCS and penicillin/streptomycin.

Cell Proliferation Assay

For 5-bromo-2'-deoxyuridine (BrdU) incorporation, quiescent cells were incubated with I3MO (1 to 5 $\mu\text{mol/L}$; kindly provided by Laurent Meijer, Roscoff, France, or by Calbiochem); Stattic, a small molecule selectively inhibiting the function of the signal transducer and activator of transcription 3 (STAT3) SH2 domain (3 to 10 $\mu\text{mol/L}$; Sigma-Aldrich); or vehicle (1% dimethyl sulfoxide [DMSO]) 30 minutes before stimulation with PDGF-BB (20 ng/mL) or thrombin (0.5 U/mL; Calbiochem). BrdU was added 1 hour later, and its incorporation was determined 23 hours after addition of the respective stimulus, according to the manufacturer's instructions (Roche Diagnostics).

Cell Cycle Analysis

Quiescent cells were preincubated with I3MO (3 or 5 $\mu\text{mol/L}$) or vehicle (1% DMSO) for 30 minutes. PDGF-BB (20 ng/mL) was added, and 16 hours (in the case of VSMCs) or 11 hours (in the case of MEFs) later, cells were harvested and the cell cycle was analyzed as described.¹⁷

[¹⁴C]L-Arginine/[¹⁴C]L-Citrulline Conversion Assay

Citrulline is produced from arginine by endothelial nitric oxide synthase (eNOS) in equimolar amounts to NO and can thus serve as a surrogate marker of NO production. The assay was performed as previously described.¹⁶

Femoral Artery Cuff Model

Male C57Bl/6 mice at 8 to 12 weeks of age were subjected to cuffing of the femoral artery. The surgical procedure was performed as described previously.¹⁸ Briefly, mice were anesthetized by intraperitoneal injection of ketamine (100 mg/kg) and xylazine (10 mg/kg), a longitudinal incision was made at the internal side of the right leg, and the right femoral artery of mice was dissected for 3 mm length from its surroundings (femoral nerve and femoral vein). A nonconstrictive polyethylene cuff (PE-50; inner diameter, 0.58 mm; outer diameter, 0.965 mm; length, 2 mm; Becton-Dickinson) was cut longitudinally, placed loosely around the right femoral artery, and filled with F-127 pluronic gel (Sigma-Aldrich) containing I3MO. This gel was prepared in advance by mixing 760 μL of cold 40% (wt/vol) F-127 pluronic gel dissolved in sterile water with 40 μL of 100 mmol/L I3MO dissolved in DMSO. Cuffs filled with F-127 pluronic gel but lacking I3MO were used in control animals. The cuff was then closed up with 2 6-0 ligature knots (USP: 6-0, Metric: 0.7, Ethicon Vicryl, Johnson & Johnson International). The skin incision was then closed with 3 sutures (USP: 6-0, Metric: 0.7, Ethicon Vicryl, Johnson & Johnson Intl.). Three, 7, 14, or 28 days after placing of the cuffs, mice were anesthetized and subsequently perfused by cardiac puncture with EDTA-PBS (1.75 mg/mL). After perfusion, a 2-cm longitudinal incision was made in the internal side of the leg, and the cuffed femoral artery was removed and embedded for cryo-sectioning. Animal care and all experimental procedures

were approved by the Animal Experimental Committee of the Medical University of Vienna and by the Austrian Ministry of Science (license no. 1321/115 and 66.009/0103-C/GI/2007).

Immunocytochemistry

Frozen sections of 5 to 7 μm thickness were fixed with precooled acetone at -20°C for 2 min and blocked with 5% normal goat serum in Primary Antibody Dilution Buffer (DAKO) for 1 hour. For quantification of VSMCs, the monoclonal (clone1A4) anti-smooth muscle actin antibody conjugated to either fluorescein isothiocyanate or Cy3 (Sigma-Aldrich) was applied for 12 hours at 4°C . For detection of phospho-STAT3, sections were pretreated with periodic acid (4 mg/100 mL), incubated overnight at 4°C with the rabbit monoclonal antibody D3A7 (Cell Signaling Technology, Danvers, Mass), washed, incubated for 1 hour at room temperature with Power Vision polymer (Immunologic, Duiven, the Netherlands), and subsequently developed with DAB/H₂O₂. For Ki-67, the rabbit monoclonal antibody clone SP6 (Thermo Scientific, Fremont, Calif) was applied overnight at 4°C followed by the Alexa 488-labeled goat anti-rabbit antibody (Invitrogen) applied for 1 hour at room temperature. After counterstaining with 4',6-diamidino-2-phenylindole (Sigma-Aldrich) for 10 minutes, the samples were mounted using Geltol (Thermo-Shandon) and visualized on an Olympus AX70 microscope (Olympus Europe GmbH). Digital images were recorded using either an F-View II or a ColorView III camera and morphometrically assessed using the software package AnalySiS Pro (Soft Imaging System).

SDS-PAGE and Immunoblotting

Serum-starved VSMCs were preincubated with I3MO (0.1 to 5 $\mu\text{mol/L}$), wortmannin, U0126, SU6656, or AG490 at the indicated concentrations or vehicle (1% DMSO) for 30 minutes and then stimulated with PDGF-BB (20 ng/mL), interferon (IFN)- γ (20 ng/mL), or thrombin (0.5 U/mL) for the indicated times. Protein isolation and immunoblotting were performed essentially as described by Haider et al.¹⁷ All antibodies used were from New England BioLabs with the exception of anti- α -tubulin (Santa Cruz Biotechnology Inc) and a horseradish peroxidase-conjugated goat anti-mouse secondary antibody (Upstate). Proteins were visualized using the ECL reagent and an LAS-3000 luminescent image analyzer (Fujifilm) with AIDA software (Raytest).

Transient Transfection

Expression vectors (1 μg), ie, Stat3 Flag pRc/CMV (Addgene plasmid 8707) encoding the wild-type or Stat3-C Flag pRc/CMV (Addgene plasmid 8722) encoding the constitutively active form of STAT3,^{19,20} were used for transfection of MEFs grown in 6-well plates using Fugene HD (Roche Diagnostics) as a transfection reagent and following the manufacturer's instructions.

Statistical Analysis

Statistical analysis was performed by *t* test or 1-way ANOVA followed by a Dunnett multiple comparison test. The number of experiments is given in the figure legends, and a probability value <0.05 was considered significant. All tests were performed using GraphPad PRISM software, version 4.03.

Results

I3MO Inhibits PDGF-BB-Induced VSMC Proliferation by Arresting Cells in G₀/G₁ Phase and Does Not Impair Endothelial Function

First, we tested I3MO for its antiproliferative activity in PDGF-activated VSMCs. Measurement of DNA synthesis via BrdU incorporation showed that PDGF-BB (20 ng/mL, 23 hours) increased DNA synthesis ≈ 3 -fold and that I3MO inhibited cell proliferation dose-dependently (Figure 1A). I3MO (3 or 5 $\mu\text{mol/L}$)-treated cells showed no signs of

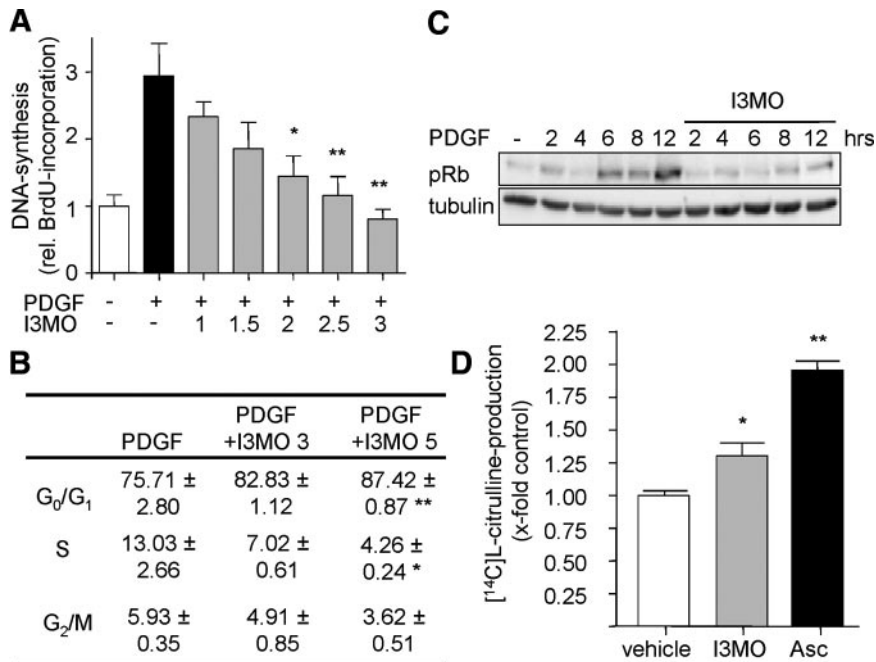


Figure 1. I3MO suppresses PDGF-BB-induced VSMC proliferation by arresting cells in G_0/G_1 phase and elevates eNOS enzymatic activity in endothelial cells. **A**, Serum-starved VSMCs were incubated with I3MO (1 to 3 μmol/L) or vehicle (1% DMSO) 30 minutes before stimulation with PDGF-BB (20 ng/mL). One hour later, BrdU (10 μmol/L) was added, and the incorporation was measured 23 hours after addition of PDGF-BB. **B**, Quiescent VSMCs were incubated with I3MO (3 or 5 μmol/L) or vehicle 30 minutes before stimulation with PDGF-BB (20 ng/mL) for 16 hours. Nuclei were stained by propidium iodide and analyzed by flow cytometry. **A** and **B**, data show the mean ± SEM; n=3; ** P <0.01, * P <0.05 versus PDGF-BB treatment (ANOVA/Dunnett). **C**, After pretreatment of VSMCs with I3MO (3 μmol/L) or vehicle for 30 minutes, cells were stimulated with PDGF-BB (20 ng/mL) for the indicated times. Hyperphosphorylated Rb was detected by Western blot analysis using a phosphospecific antibody for the S807/811 residue; tubulin was used as loading control. One representative immunoblot out of 3 experiments is shown. **D**,

EA.hy926 cells were treated with I3MO (3 μmol/L), vehicle (0.1% DMSO), or the positive control ascorbic acid (Asc, 100 μmol/L) for 24 hours. eNOS enzyme activity was determined by the [¹⁴C]-arginine/[¹⁴C]-citrulline conversion assay. [¹⁴C]-citrulline production was normalized to solvent control. Bars represent the mean ± SEM of 3 independent experiments performed in quadruplicate. ** P <0.01, * P <0.05 versus vehicle treatment (ANOVA/Dunnett).

apoptosis as measured by the absence of nuclei with a subdiploid DNA content or nuclear fragmentation (data not shown). Cell cycle analysis by flow cytometry revealed an arrest of I3MO (3 or 5 μmol/L)-treated VSMCs in G_0/G_1 phase (Figure 1B). To exclude that I3MO causes a DNA replication block in early S phase, which is difficult to distinguish from a G_0/G_1 arrest by flow cytometry, we arrested cells using the reversible DNA-polymerase inhibitor aphidicolin (1 μmol/L) in early S phase. Subsequent treatment of released cells (after washout of aphidicolin) with I3MO did not prevent DNA synthesis, as shown by newly incorporated BrdU (Supplemental Figure I). Hyperphosphorylation of the retinoblastoma protein (Rb), an important regulator at the G_1/S phase transition, is required for S phase entry.²¹ As expected, stimulation of VSMCs with PDGF-BB alone led to a time-dependent increase in phosphorylation of Rb on S807/811, first detectable after 6 hours. Cells treated with I3MO kept Rb in a hypophosphorylated state (Figure 1C), again confirming cell cycle arrest in G_0/G_1 phase.

eNOS represents an enzyme crucial for antiatherosclerotic endothelial function²² and for NO-dependent inhibition of VSMC proliferation.^{23,24} To exclude a negative effect of I3MO on endothelial function as judged by eNOS activity, human endothelial EA.hy926 cells were exposed to I3MO (3 μmol/L) or, as a positive control, to ascorbic acid (100 μmol/L) for 24 hours, and L-citrulline production was measured. Most interestingly, I3MO slightly but significantly increased eNOS activity to ≈1.3-fold (Figure 1D). Moreover, I3MO had no negative influence on endothelial cell viability (Supplemental Figure II).

I3MO Prevents Neointima Formation in a Mouse Femoral Artery Cuff Model

Next, we examined whether I3MO reduces neointima formation in vivo. The femoral artery cuff model has been used previously to study the process of restenosis in mice.^{25,26} To examine the effect of locally applied I3MO on cuff-induced stenosis of an artery, we dissolved the substance in F-127 pluronic gel and placed the gel into the cuff surrounding the femoral artery. Twenty-eight days after placing the cuff, we observed an inhibitory effect of I3MO on cuff-induced neointima formation. As depicted in Figure 2A, 2B, and 2D, I3MO was capable of attenuating the development of a neointima significantly without affecting the thickness of the media. In consequence, the neointima/media ratio was significantly reduced by more than 50% (Figure 2C).

I3MO Suppresses Activation of STAT3 but Not of Mitogen-Activated Protein Kinases and Akt

We then analyzed the molecular mediators of the antiproliferative activity of I3MO in VSMCs. In the presence of calf serum (10%), no significant inhibition of cell proliferation was observed in response to 1 to 10 μmol/L I3MO (data not shown). This indicates that I3MO at concentrations below 10 μmol/L does not block cell cycle entry via a direct inhibition of CDKs but rather interferes with a step further upstream in the mitogenic response to PDGF.

The kinase Akt and the mitogen-activated protein kinases Erk1/2 or p38^{MAPK} are critically involved in VSMC proliferation.²⁷ As shown in Figure 3A (upper panel), I3MO (3 or 5 μmol/L) failed to reduce PDGF-induced phosphorylation of any of these kinases, whereas the phosphatidylinositol

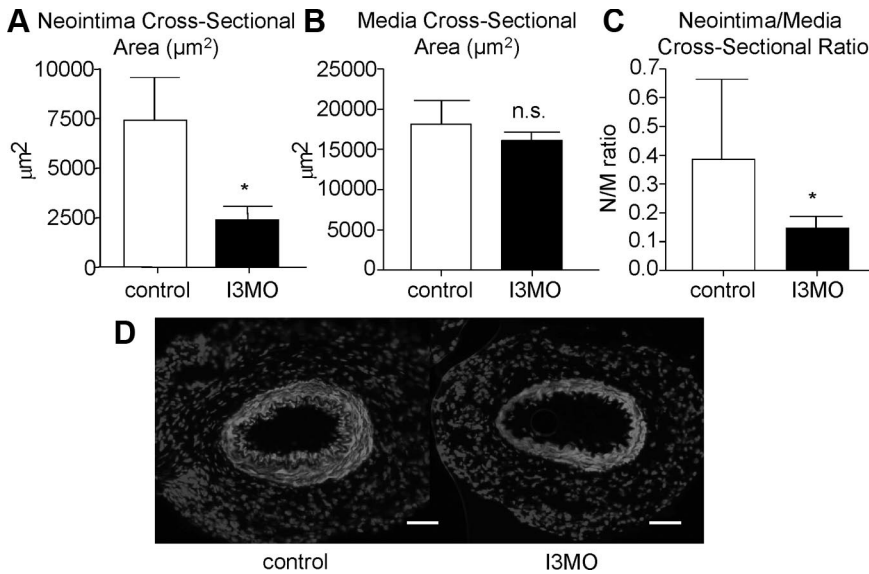


Figure 2. I3MO inhibits neointima formation in vivo. A nonconstrictive polyethylene cuff filled with F-127 pluronic gel containing I3MO or vehicle (control) was placed loosely around the right femoral artery of mice. A to C, Quantitative analysis of the neointima cross-sectional area (A), the media cross-sectional area (B), and the neointima to media cross-sectional ratio (C) at day 28 after cuff placement. Graphs indicate mean \pm SEM; n=7; * P <0.05 versus vehicle control (unpaired t test). D, Representative microscopic photographs of immunohistochemistry staining for smooth muscle actin in femoral arteries; scale bars, 50 μ m.

3-kinase inhibitor wortmannin and the MEK1/2 inhibitor U0126 inhibited activation of Akt and Erk1/2, respectively. Neither treatment with PDGF-BB nor treatment with I3MO changed the total protein levels of Akt, Erk1/2, or p38^{MAPK}. On ligand binding, tyrosine phosphorylation of the PDGF receptor was only moderately impaired by I3MO (Supplemental Figure III). These data exclude the intrinsic tyrosine kinase of PDGF receptor as the main and immediate target of I3MO.

Signal transducer and activator of transcription 3 (STAT3) is thought to participate in PDGF-induced cell proliferation.^{28,29} Indeed, stimulation of VSMCs with PDGF-BB (20 ng/mL, 10 minutes) led to a strong phosphorylation of Y705 in STAT3, a critical residue for dimerization of STAT3 and subsequent translocation into the nucleus. The Src family kinase inhibitor SU6656 but not the JAK2 inhibitor AG490 was able to abrogate activation of STAT3, indicating a Src-dependent but JAK2-independent phosphorylation of STAT3 on PDGF treatment in VSMCs. Preincubation with I3MO (3 or 5 μ mol/L) completely abolished phosphorylation

of Y705 (Figure 3A, lower panel). Total amounts of STAT3 were not affected by I3MO.

I3MO Inhibits STAT3 Phosphorylation in a Dose-Dependent but Stimulus-Independent Manner

I3MO suppressed PDGF-induced STAT3 phosphorylation dose-dependently, first observed at a concentration of 0.3 μ mol/L (Figure 3B, upper panel) To examine whether STAT3 inhibition by I3MO is stimulus dependent, we activated VSMCs with IFN- γ (20 ng/mL), a mediator of proatherogenic processes^{30,31} and known activator of STAT proteins.³² Treatment with IFN- γ resulted in a clear increase in phosphorylation of Y705 (Figure 3B, middle panel), which was inhibited by I3MO in a dose-dependent manner. Moreover, STAT3 phosphorylation induced by thrombin (0.5 U/mL), another potent mitogen in VSMCs,³³ was also completely blunted by I3MO (Figure 3B, lower panel). I3MO (3 μ mol/L) also prevented the translocation of the active, phosphorylated form of STAT3 into the nucleus (Supplemental Figure IVA and IVB).

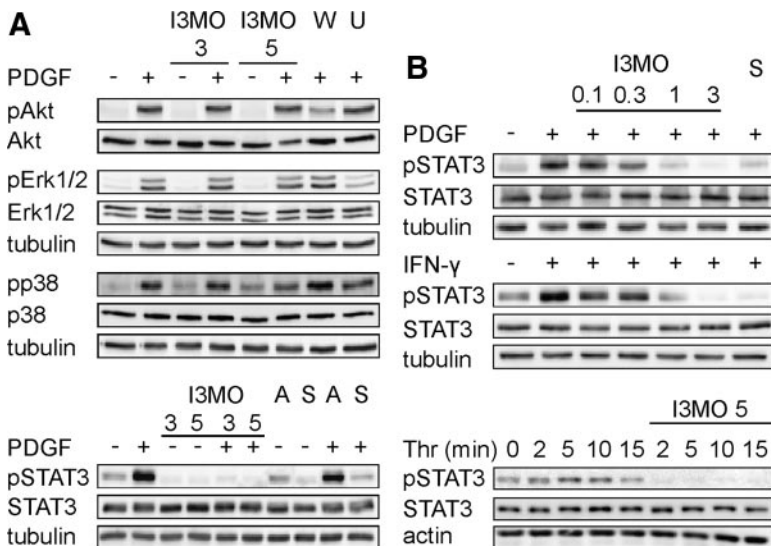
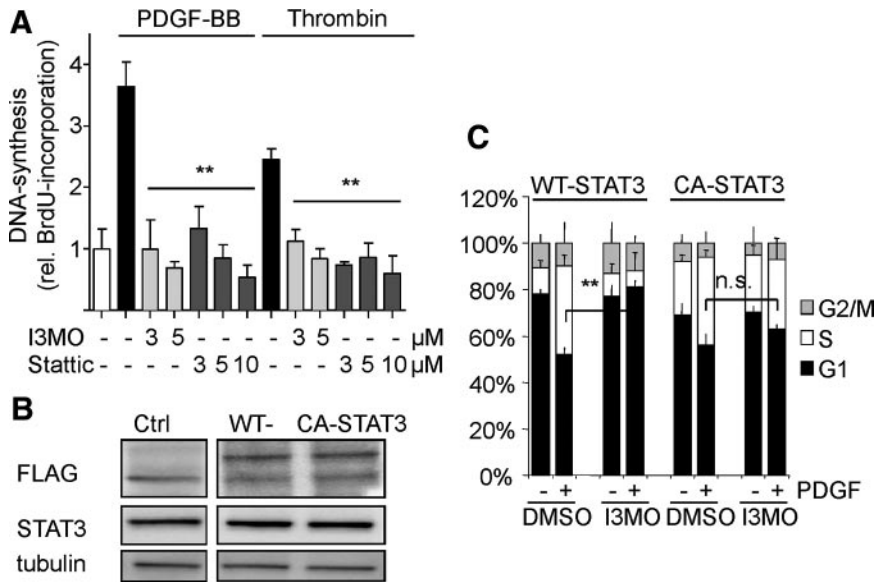


Figure 3. I3MO abolishes STAT3 phosphorylation in a dose-dependent but stimulus-independent manner without affecting Akt, Erk1/2, or p38^{MAPK}. A, Quiescent VSMCs were preincubated with either I3MO (3 or 5 μ mol/L), wortmannin (W, 50 nmol/L), U0126 (U, 10 μ mol/L), AG490 (A, 10 μ mol/L), SU6656 (S, 2 μ mol/L), or vehicle (1% DMSO) for 30 minutes and stimulated with PDGF-BB (20 ng/mL), IFN- γ (20 ng/mL) for 10 minutes. Immunoblotting was performed using specific antibodies against phosphorylated (pAkt [S473], pErk1/2 [T202/Y204], pp38^{MAPK} [T180/Y182], pSTAT3 [Y705]) and unphosphorylated proteins. B, Serum-starved cells were pretreated with either I3MO as indicated or vehicle (1% DMSO) for 30 minutes and stimulated with PDGF-BB (20 ng/mL), IFN- γ (20 ng/mL) for 10 minutes, or thrombin (Thr, 0.5 U/mL) for the indicated periods of time. Western blot analysis was performed using specific antibodies against phosphorylated (Y705) and unphosphorylated STAT3. A and B, Representative immunoblots out of 3 experiments are shown; tubulin or actin was used as loading control.



staining and flow cytometry for cell cycle analysis. Graph shows mean values \pm SEM out of 3 experiments; ** $P < 0.01$ (Student *t* test [cells in S phase after stimulation: DMSO versus I3MO]).

Finally, to rule out that inhibition of STAT3 phosphorylation occurs only in the first hour after stimulation, we performed long-term experiments up to a period of 18 hours. I3MO (3 or 5 μ mol/L) kept STAT3 hypophosphorylated throughout the entire incubation time (Supplemental Figure V).

STAT3 Inhibition Leads to Inhibition of Cell Proliferation

To underline that inhibition of STAT3 phosphorylation is sufficient to inhibit VSMC proliferation, we used Stattic, a selective inhibitor of STAT3 phosphorylation and dimerization.³⁴ Incubation with either Stattic or I3MO prevented PDGF- and thrombin-mediated VSMC proliferation in a dose-dependent manner as evidenced by reduced BrdU incorporation (Figure 4A). Like I3MO, Stattic did not inhibit ERK1/2, p38^{MAPK} or AKT phosphorylation (data not shown). Moreover, MEFs expressing a constitutively active form of STAT3 (Figure 4B) were able to escape the cell cycle arrest induced by I3MO in cells expressing wild-type STAT3. Whereas I3MO significantly reduced the percentage of wild-type cells moving to S phase after PDGF stimulation, constitutively active cells remained unaffected by I3MO (Figure 4C). These findings underline the notion of activated STAT3 as an important mediator of VSMC proliferation^{33,35} and suggest that inhibition of STAT3 phosphorylation is indeed the molecular mechanism underlying the antiproliferative effect of I3MO.

I3MO Inhibits STAT3 Phosphorylation In Vivo

In a next step, our goal was to confirm the correlation between reduced STAT3 phosphorylation and reduced VSMC proliferation in our *in vivo* model. By immunocytochemical staining, we could show that I3MO-treated arteries displayed a reduced number of phosphoSTAT3⁺ cells at days 3, 7, and 14 after cuff placement compared with arteries

treated with vehicle (Figure 5A and 5B). The observed decrease in STAT3 phosphorylation was reflected by a reduced number of proliferating Ki67-positive cells (Figure 5C and 5D).

These data strongly indicate that the phosphorylation of STAT3 serves as a major target of I3MO both *in vitro* and *in vivo*.

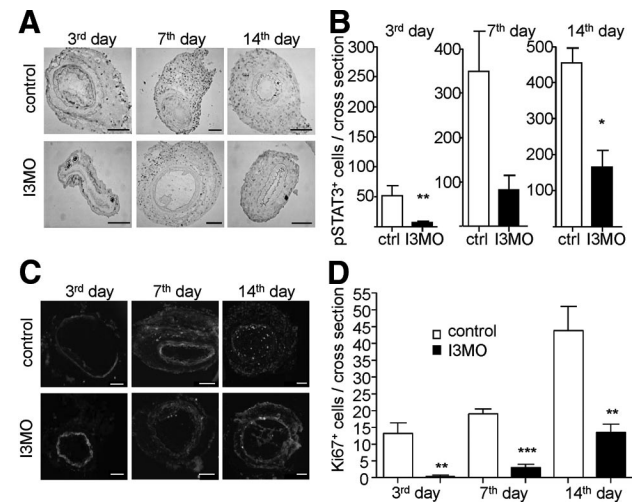


Figure 5. I3MO reduces STAT3 phosphorylation and proliferation in cuffed arteries *in vivo*. **A**, Representative images of immunohistochemical phospho-STAT3 (pSTAT3) detection on cross-sections of femoral arteries, cuffed for 3, 7, or 14 days in the presence or absence of I3MO. **B**, Quantification of pSTAT3-positive cells 3, 7, and 14 days after I3MO treatment. **C**, Immunofluorescent detection of proliferating Ki67-positive cells (green), smooth muscle cell actin (red), and nuclei (blue). **D**, Quantification of proliferating cells (Ki67) at days 3, 7, and 14 in I3MO-treated and control (DMSO)-treated cuffed arteries. Bars represent mean values \pm SEM of experiments performed on at least 4 mice per group; *** $P < 0.001$, ** $P < 0.01$, * $P < 0.05$ (Student *t* test); scale bars, 50 μ m.

Discussion

The present study shows that I3MO, a derivative of the natural product indirubin, potentially inhibits DNA synthesis in PDGF-activated VSMCs by arresting cells in the G₁ phase of the cell cycle and significantly reduces neointima formation when applied locally in an animal cuff-induced neointima model. In contrast to previous studies that characterized I3MO as a potent CDK inhibitor *in vitro*,^{6–9} we show that I3MO acts upstream of CDKs by completely abrogating PDGF-induced STAT3 activation in VSMCs. Importantly, I3MO also inhibited IFN- γ - and thrombin-mediated STAT3 activation, whereas none of the typical growth factor-induced signaling pathways, such as Akt or the mitogen-activated protein kinases Erk1/2 or p38^{MAPK}, were affected. Interestingly, in the mouse femoral artery cuff model also, where I3MO reduced neointima formation, the number of phospho-STAT3-positive cells was reduced, correlating with a reduced number of proliferating cells. Endothelial function as judged by eNOS activity was not negatively affected by I3MO. The observed strong interference of the known CDK inhibitor I3MO with the STAT3 signaling pathway in VSMCs was rather unexpected, although a previous study has shown that some indirubin derivatives are able to block constitutive STAT3 signaling in tumor cells.¹² In tumorigenesis, a role for STAT proteins is quite well established.³⁶ However, less is known regarding STAT proteins and their role in cardiovascular diseases. With respect to neointima formation and vascular remodeling, Seki et al showed that JAKs and STATs are induced in medial and neointimal VSMCs after vascular injury and that JAK inhibition leads to reduced STAT phosphorylation, reduced neointimal VSMC replication, and neointima formation.³⁷ The same group also demonstrated that adenoviral overexpression of a dominant negative STAT3 in a balloon-injury artery model reduces neointimal VSMC proliferation and neointima formation.³⁵ A more recent article by Wang et al suggested a strong role for the interleukin-6/gp130/STAT3 signaling in vascular remodeling and neointima formation.³⁸ Moreover, STAT3 activation has recently been shown to be involved in VSMC inflammation and vascular remodeling on injury.³⁹ All these studies indicate that in fact inhibition of the JAK-STAT pathway could affect neointima formation. In our study, we confirmed a role for STAT3 inhibition by I3MO in reducing neointima formation *in vivo* and by inhibiting PDGF-induced VSMC proliferation *in vitro*.

I3MO abrogated not only PDGF-induced STAT3 phosphorylation but also STAT3 activation in response to IFN- γ and thrombin. This is of special importance because the proinflammatory cytokine IFN- γ plays a central role in atherosclerosis, restenosis, and neointima formation.^{40–42} Although different mechanisms for the mitogenic and motogenic activity of thrombin for VSMCs were suggested, there are data indicating that STAT3 also plays a role for thrombin-induced cell motility and proliferation.^{43–45}

Interference with the STAT signaling pathway is a mechanism that differs considerably from those shown for established vascular antiproliferative drugs, such as rapamycin or paclitaxel. Paclitaxel inhibits microtubule dynamics, leading predominantly to M phase arrest. Because paclitaxel inter-

feres at a stage of the cell cycle where cells are supposed to divide, proapoptotic mechanisms are likely to occur.⁵ In combination with impaired reendothelialization, this might be detrimental for arterial wound healing, and it possibly increases the risk for thrombosis.⁵ In contrast, I3MO did not induce apoptosis in the effective antiproliferative range of concentrations. Rapamycin inhibits mTOR, the mammalian target of rapamycin, arresting cells in G₁ phase via elevated levels of p27^{KIP}, a CDK inhibitor. In addition, rapamycin has an immunosuppressive activity that is thought to be beneficial for the local suppression of inflammatory responses.⁵ I3MO, similar to rapamycin, arrests VSMCs in G₁ phase and seems to have an antiinflammatory activity by interfering with IFN- γ signaling and inhibiting tumor necrosis factor- α -induced nuclear factor κ B activation, as demonstrated in human leukemic cells.¹⁴ We show here that I3MO significantly reduces neointima formation in a mouse femoral artery model by inhibition of phosphorylation of STAT3 as demonstrated *in vitro* and *in vivo*, suggesting I3MO as a promising lead compound that warrants further investigation regarding its potential use to prevent neointima formation.

Acknowledgments

We thank Dr Laurent Meijer (Centre National de la Recherche Scientifique, Station Biologique, Roscoff, France) for providing I3MO. In addition, we would like to dedicate this work to our deceased colleague and coauthor Dr Bernd R. Binder.

Sources of Funding

This study was supported by grants from the European Union as part of the European Union project Pro-KinaseResearch (Project No. LSHB-CT-2004-503467) (to V.M.D.), as well as from the Austrian Science Fund (NFN S107-B03 “DNIT—Drugs From Nature Targeting Inflammation”) (to V.M.D. and B.R.B.) and the Leducq Foundation LINK Transatlantic Network (to B.R.B.). Part of this work (B.R.B.) was performed also within the European Union 6th Framework Program European Vascular Genomics Network (Project No. LSHM-CT-2003-503254).

Disclosures

None.

References

1. Breuss JM, Cejna M, Bergmeister H, Kadl A, Baumgartl G, Steurer S, Xu Z, Koshelnick Y, Lipp J, De Martin R, Losert U, Lammer J, Binder BR. Activation of nuclear factor- κ B significantly contributes to lumen loss in a rabbit iliac artery balloon angioplasty model. *Circulation*. 2002;105:633–638.
2. Dzau VJ, Braun-Dullaeus RC, Sedding DG. Vascular proliferation and atherosclerosis: new perspectives and therapeutic strategies. *Nat Med*. 2002;8:1249–1256.
3. Costa MA, Simon DI. Molecular basis of restenosis and drug-eluting stents. *Circulation*. 2005;111:2257–2273.
4. Maisel WH. Unanswered questions: drug-eluting stents and the risk of late thrombosis. *N Engl J Med*. 2007;356:981–984.
5. Wessely R, Schomig A, Kastrati A. Sirolimus and Paclitaxel on polymer-based drug-eluting stents: similar but different. *J Am Coll Cardiol*. 2006;47:708–714.
6. Hoessel R, Leclerc S, Endicott JA, Nobel ME, Lawrie A, Tunnah P, Leost M, Damiens E, Marie D, Marko D, Niederberger E, Tang W, Eisenbrand G, Meijer L. Indirubin, the active constituent of a Chinese antileukaemia medicine, inhibits cyclin-dependent kinases. *Nat Cell Biol*. 1999;1:60–67.
7. Meijer L, Skaltsounis AL, Magiatis P, Polychronopoulos P, Knockaert M, Leost M, Ryan XP, Vonica CA, Brivanlou A, Dajani R, Crovace C, Tarricone C, Musacchio A, Roe SM, Pearl L, Greengard P. GSK-3-

- selective inhibitors derived from Tyrian purple indirubins. *Chem Biol*. 2003;10:1255–1266.
8. Polychronopoulos P, Magiatis P, Skaltsounis AL, Myrianthopoulos V, Mikros E, Tarricone A, Musacchio A, Roe SM, Pearl L, Leost M, Greengard P, Meijer L. Structural basis for the synthesis of indirubins as potent and selective inhibitors of glycogen synthase kinase-3 and cyclin-dependent kinases. *J Med Chem*. 2004;47:935–946.
 9. Ferandin Y, Bettayeb K, Kritsanida M, Lozach O, Polychronopoulos P, Magiatis P, Skaltsounis AL, Meijer L. 3'-Substituted 7-halogenoindirubins, a new class of cell death inducing agents. *J Med Chem*. 2006;49:4638–4649.
 10. Damiens E, Baratte B, Marie D, Eisenbrand G, Meijer L. Anti-mitotic properties of indirubin-3'-monoxime, a CDK/GSK-3 inhibitor: induction of endoreplication following prophase arrest. *Oncogene*. 2001;20:3786–3797.
 11. Knockaert M, Blondel M, Bach S, Leost M, Elbi C, Hager GL, Nagy SR, Han D, Denison M, Ffrench M, Ryan XP, Magiatis P, Polychronopoulos P, Greengard P, Skaltsounis L, Meijer L. Independent actions on cyclin-dependent kinases and aryl hydrocarbon receptor mediate the antiproliferative effects of indirubins. *Oncogene*. 2004;23:4400–4412.
 12. Nam S, Buettner R, Turkson J, Kim D, Cheng JQ, Muehlbeyer S, Hippe F, Vatter S, Merz KH, Eisenbrand G, Jove R. Indirubin derivatives inhibit Stat3 signaling and induce apoptosis in human cancer cells. *Proc Natl Acad Sci U S A*. 2005;102:5998–6003.
 13. Ribas J, Bettayeb K, Ferandin Y, Knockaert M, Garofe-Ochoa X, Totzke F, Schachtele C, Mester J, Polychronopoulos P, Magiatis P, Skaltsounis AL, Boix J, Meijer L. 7-Bromoindirubin-3'-oxime induces caspase-independent cell death. *Oncogene*. 2006;25:6304–6318.
 14. Sethi G, Ahn KS, Sandur SK, Lin X, Chaturvedi MM, Aggarwal BB. Indirubin enhances tumor necrosis factor-induced apoptosis through modulation of nuclear factor-kappa B signaling pathway. *J Biol Chem*. 2006;281:23425–23435.
 15. Haider UG, Roos TU, Kontaridis MI, Neel BG, Sorescu D, Griendling KK, Vollmar AM, Dirsch VM. Resveratrol inhibits angiotensin II- and epidermal growth factor-mediated Akt activation: role of Gab1 and Shp2. *Mol Pharmacol*. 2005;68:41–48.
 16. Leikert JF, Rathel TR, Wohlfart P, Cheyner V, Vollmar AM, Dirsch VM. Red wine polyphenols enhance endothelial nitric oxide synthase expression and subsequent nitric oxide release from endothelial cells. *Circulation*. 2002;106:1614–1617.
 17. Haider UG, Sorescu D, Griendling KK, Vollmar AM, Dirsch VM. Resveratrol increases serine15-phosphorylated but transcriptionally impaired p53 and induces a reversible DNA replication block in serum-activated vascular smooth muscle cells. *Mol Pharmacol*. 2003;63:925–932.
 18. Moroi M, Zhang L, Yasuda T, Virmani R, Gold HK, Fishman MC, Huang PL. Interaction of genetic deficiency of endothelial nitric oxide, gender, and pregnancy in vascular response to injury in mice. *J Clin Invest*. 1998;101:1225–1232.
 19. Horvath CM, Wen Z, Darnell JE. A STAT protein domain that determines DNA sequence recognition suggests a novel DNA-binding domain. *Genes Dev*. 1995;9:984–994.
 20. Bromberg JF, Wrzeszczynska MH, Devgan G, Zhao Y, Pestell RG, Albanese C, Darnell JE. Stat3 as an oncogene. *Cell*. 1999;98:295–303.
 21. Sherr CJ. Cancer cell cycles. *Science*. 1996;274:1672–1677.
 22. Napoli C, Ignarro LJ. Nitric oxide and atherosclerosis. *Nitric Oxide*. 2001;5:88–97.
 23. Cooney R, Hynes SO, Sharif F, Howard L, O'Brien T. Effect of gene delivery of NOS isoforms on intimal hyperplasia and endothelial regeneration after balloon injury. *Gene Ther*. 2007;14:396–404.
 24. Cooney R, Hynes SO, Duffy AM, Sharif F, O'Brien T. Adenoviral-mediated gene transfer of nitric oxide synthase isoforms and vascular cell proliferation. *J Vasc Res*. 2006;43:462–472.
 25. Tsukada S, Iwai M, Nishiu J, Itoh M, Tomoike H, Horiuchi M, Nakamura Y, Tanaka T. Inhibition of experimental intimal thickening in mice lacking a novel G-protein-coupled receptor. *Circulation*. 2003;107:313–319.
 26. Engelse MA, Arkenbout EK, Pannekoek H, de Vries CJ. Activin and TR3 orphan receptor: two 'atheroprotective' genes as evidenced in dedicated mouse models. *Clin Exp Pharmacol Physiol*. 2003;30:894–899.
 27. Berk BC. Vascular smooth muscle growth: autocrine growth mechanisms. *Physiol Rev*. 2001;81:999–1030.
 28. Bowman T, Broome MA, Sinibaldi D, Wharton W, Pledger WJ, Sedivy JM, Irby R, Yeatman T, Courtneidge SA, Jove R. Stat3-mediated Myc expression is required for Src transformation and PDGF-induced mitogenesis. *Proc Natl Acad Sci U S A*. 2001;98:7319–7324.
 29. Simon AR, Takahashi S, Severgnini M, Fanburg BL, Cochran BH. Role of the JAK-STAT pathway in PDGF-stimulated proliferation of human airway smooth muscle cells. *Am J Physiol Lung Cell Mol Physiol*. 2002;282:L1296–L1304.
 30. Tellides G, Tereb DA, Kirkiles-Smith NC, Kim RW, Wilson JH, Schechner JS, Lorber MI, Pober JS. Interferon- γ elicits arteriosclerosis in the absence of leukocytes. *Nature*. 2000;403:207–211.
 31. Harvey EJ, Ramji DP. Interferon- γ and atherosclerosis: pro- or anti-atherogenic? *Cardiovasc Res*. 2005;67:11–20.
 32. Stark GR, Kerr IM, Williams BR, Silverman RH, Schreiber RD. How cells respond to interferons. *Annu Rev Biochem*. 1998;67:227–264.
 33. Madamanchi NR, Li S, Patterson C, Runge MS. Thrombin regulates vascular smooth muscle cell growth and heat shock proteins via the JAK-STAT pathway. *J Biol Chem*. 2001;276:18915–18924.
 34. Schust J, Sperl B, Hollis A, Mayer TU, Berg T. Stattic: a small-molecule inhibitor of STAT3 activation and dimerization. *Chem Biol*. 2006;13:1235–1242.
 35. Shibata R, Kai H, Seki Y, Kato S, Wada Y, Hanakawa Y, Hashimoto K, Yoshimura A, Imaizumi T. Inhibition of STAT3 prevents neointima formation by inhibiting proliferation and promoting apoptosis of neointimal smooth muscle cells. *Hum Gene Ther*. 2003;14:601–610.
 36. Yu H, Jove R. The STATs of cancer: new molecular targets come of age. *Nature Rev*. 2004;4:97–105.
 37. Seki Y, Kai H, Shibata R, Nagata T, Yasukawa H, Yoshimura A, Imaizumi T. Role of the JAK/STAT pathway in rat carotid artery remodeling after vascular injury. *Circ Res*. 2000;87:12–18.
 38. Wang D, Liu Z, Li Q, Karpurapu M, Kundumani-Sridharan V, Cao H, Dronadula N, Rizvi F, Bajpai AK, Zhang C, Muller-Newen G, Harris KW, Rao GN. An essential role for gp130 in neointima formation following arterial injury. *Circ Res*. 2007;100:807–816.
 39. Kovacic JC, Gupta R, Lee AC, Ma M, Fang F, Tolbert CN, Walts AD, Beltran LE, San H, Chen G, St Hilaire C, Boehm M. Stat3-dependent acute Rantes production in vascular smooth muscle cells modulates inflammation following arterial injury in mice. *J Clin Invest*. 2010;120:303–314.
 40. Leon ML, Zuckerman SH. Gamma interferon: a central mediator in atherosclerosis. *Inflamm Res*. 2005;54:395–411.
 41. Zohlhofer D, Richter T, Neumann F, Nuhrenberg T, Wessely R, Brandl R, Murr A, Klein CA, Baeuerle PA. Transcriptome analysis reveals a role of interferon- γ in human neointima formation. *Mol Cell*. 2001;7:1059–1069.
 42. Kusaba K, Kai H, Koga M, Takayama N, Ikeda A, Yasukawa H, Seki Y, Egashira K, Imaizumi T. Inhibition of intrinsic interferon- γ function prevents neointima formation after balloon injury. *Hypertension*. 2007;49:909–915.
 43. Maruyama I, Shigeta K, Miyahara H, Nakajima T, Shin H, Ide S, Kitajima I. Thrombin activates NF- κ B through thrombin receptor and results in proliferation of vascular smooth muscle cells: role of thrombin in atherosclerosis and restenosis. *Ann NY Acad Sci*. 1997;811:429–436.
 44. Wang Z, Castresana MR, Newman WH. Reactive oxygen species-sensitive p38 MAPK controls thrombin-induced migration of vascular smooth muscle cells. *J Mol Cell Cardiol*. 2004;36:49–56.
 45. Dronadula N, Liu Z, Wang C, Cao H, Rao GN. STAT-3-dependent cytosolic Phospholipase A₂ expression is required for thrombin-induced vascular smooth muscle cell motility. *J Biol Chem*. 2005;280:3112–3120.

Online Data Supplement

Supplemental Material

Materials

Calf serum, phenol red-free Dulbecco's modified Eagle's medium containing 4.5 g/L glucose, L-glutamine, penicillin/streptomycin and HAT supplement (100 $\mu\text{mol/L}$ hypoxanthine, 0.4 $\mu\text{mol/L}$ aminopterin, 16 $\mu\text{mol/L}$ thymidine) were obtained from Lonza (Belgium), trypsin (1:250) and fetal bovine serum from Gibco via Invitrogen (CA, USA). Recombinant human PDGF-BB was purchased from Bachem (Germany), recombinant rat IFN- γ from Pepro Tech (United Kingdom), and thrombin was purchased from Calbiochem (CA, USA). Wortmannin and U0126 were obtained from New England BioLabs (MA, USA), AG490 and SU6656 from Calbiochem (CA, USA), propidium iodide (PI) from Fluka (Switzerland).

Antibodies against phospho-Akt (S⁴⁷³), phospho-Erk1/2 MAPK (T²⁰²/Y²⁰⁴), phospho-p38^{MAPK} (T¹⁸⁰/Y¹⁸²), phospho-STAT3 (Y⁷⁰⁵), phospho-retinoblastoma protein (S^{807/811}), phospho-tyrosine, phospho-PDGFR (Y579/581 and Y857) as well as Akt, Erk1/2, p38^{MAPK}, STAT3, and the horseradish peroxidase-conjugated goat anti-rabbit secondary antibody were from New England BioLabs (MA, USA), anti- α -tubulin and actin were from Santa Cruz (CA, USA) and horseradish peroxidase-conjugated goat anti-mouse secondary antibody from Upstate (VA, USA). Antibody against FLAG was purchased from Sigma-Aldrich (MO, USA). Monoclonal anti-smooth muscle actin-FITC (Sigma-Aldrich, MO, USA) and DAPI (4',6-diamidino-2-phenylindole; Vector Laboratories, CA, USA) were obtained as indicated. To account for unspecific binding, purified non-immune mouse IgG (Sigma-Aldrich, MO, USA) was used in controls.

CompleteTM and Cell Proliferation ELISA, BrdU (chemiluminescence) were obtained from Roche Diagnostics (Germany). Indirubin-3'-monoxime was kindly provided by Laurent Meijer (Roscoff, France) or purchased from Calbiochem (CA, USA). All other reagents were purchased from Sigma-Aldrich (MO, USA).

Cell Culture

Vascular smooth muscle cells (VSMCs) were isolated from male Sprague-Dawley rat thoracic aortas by enzymatic digestion as described previously.¹ Cells were cultured (37°C and 5% CO₂) in phenol red-free Dulbecco's modified Eagle's medium supplemented with 2 mmol/L glutamine, 100 units/mL penicillin, 100 µg/mL streptomycin and 10% calf serum, passaged twice a week by harvesting with trypsin/EDTA and seeded into 75-cm² flasks. For experiments, cells between passage 7 and 15 were used at 50, 70 or 90% confluence. The human endothelial cell line EA.hy926 (kindly provided by Dr. C.-J. Edgell, University of North Carolina, Chapel Hill, NC) was cultivated like VSMCs except for 10% fetal bovine serum and additional HAT supplement (100 µmol/L hypoxanthine, 0.4 µmol/L aminopterin, 16 µmol/L thymidine) till passage 30. For experiments, cells were seeded in 6-well plates at a density of 5 x 10⁵ cells/well and were stimulated at confluency, approximately after 72 hrs. Porcine aortic endothelial cells were cultivated in Ham's F12 medium supplemented with 10 % fetal bovine serum, 100 units/mL penicillin and 100 µg/mL streptomycin.

[¹⁴C]L-arginine/[¹⁴C]L-citrulline Conversion Assay

Citrulline is produced from arginine by endothelial nitric oxide synthase (eNOS) in equimolar amounts to NO and can thus serve as a surrogate marker of NO production. Briefly, EA.hy926 cells stimulated for 24 hrs with vehicle (DMSO 0.1%), I3MO (3 µmol/L) or the positive control ascorbic acid (100 µmol/L) were equilibrated in HEPES buffer, then 0.32 µmol/L [¹⁴C]L-arginine (313 Ci/mmol) and 1 µmol/L ionomycin were added. After lysing and extracting cells with ethanol/water, extracts were dried under vacuum (SPD 1010 SpeedVac, Thermo Savant) and resolved in water/methanol (1:1). After separation from [¹⁴C]L-arginine by thin layer chromatography (Polygram SIL N-HR, Machery Nagel, Austria), [¹⁴C]L-citrulline was quantified by autoradiography in a phosphorimager (BAS-1800II, Fujifilm, Japan). AIDA software (raytest USA Inc., NC, USA) was used for densitometric analysis.

Cell Proliferation and Viability Assays

For BrdU-incorporation cells were seeded at a density of 3×10^4 cells/well in 96-well plates, grown over night with 10% calf serum and then rendered quiescent by serum withdrawal for 24 hrs. Medium was changed and cells were incubated with indirubin-3'-monoxime (I3MO, 1-3 $\mu\text{mol/L}$) or vehicle (DMSO 1%) 30 min prior to stimulation with PDGF-BB (20 ng/mL) or 10% calf serum (CS). One hr later BrdU at a final concentration of 10 $\mu\text{mol/L}$ was added and BrdU-incorporation was determined on the Tecan GENios ProTM luminometer (Mannedorf, Switzerland) 23 hrs after addition of PDGF-BB or CS, respectively, according to the instructions of the Cell Proliferation ELISA Kit (Roche Diagnostics, Germany). Viability was assessed by automated determination of the percentage of cells that are able to exclude Trypan Blue with a ViCellTM instrument (Beckman Coulter)

Cell Cycle Analysis

The percentage of cells in each cell cycle phase was obtained based on the flow cytometric analysis of propidium iodide (PI)-stained nuclear DNA. To arrest cells in G₁-phase of the cell cycle, cells at 70% confluence were serum starved for 24 hrs and then preincubated with I3MO (3 and 5 $\mu\text{mol/L}$) or vehicle (DMSO 1%) for 30 min. PDGF-BB (20 ng/mL) was added and 16 hrs later, cells were trypsinized, washed once with PBS, and incubated in a hypotonic PI solution containing 0.1% (v/v) Triton X-100, 0.1% (w/v) sodium citrate, and 50 $\mu\text{g/mL}$ PI over night. 10,000 cells were analyzed by flow cytometry (FACSCaliburTM, BD Biosciences, Germany) by setting markers manually on the phases of the cell cycle.

To characterize cells that are actively synthesizing DNA depending on their cell cycle position, cells were seeded at a density of 8×10^4 cells/well in 6-well plates and rendered quiescent by serum withdrawal for four days. After changing the medium and adding vehicle (DMSO 1%), cells were stimulated with PDGF-BB (20 ng/mL). Four hrs later, the reversible DNA-polymerase inhibitor aphidicolin (1 $\mu\text{mol/L}$) was added to arrest the cells in early S-

phase. After another 15 hrs of incubation aphidicolin was removed by washing the cells once with warm PBS before adding fresh medium containing PDGF-BB and, depending on the treatment, again aphidicolin (2 $\mu\text{mol/L}$) or I3MO (3 or 5 $\mu\text{mol/L}$) or vehicle (DMSO 1%). Cells were incubated for 10 hrs and during the last 30 min pulse labelled with 10 $\mu\text{mol/L}$ BrdU. Subsequently, cells were harvested by trypsinization and processed as described by the manufacturer of the FITC BrdU Flow Kit (BD Biosciences Pharmingen, CA, USA). Incorporated BrdU was made detectable by immunostaining with a FITC-conjugated anti-BrdU antibody; additionally, nuclear DNA was stained with 7-aminoactinomycin D. The emitted fluorescence of 10,000 cells was monitored by flow cytometry.

SDS-PAGE and Immunoblotting

Cells at 70 to 90% confluence were serum starved for 24 hrs, preincubated with I3MO (0.1-5 $\mu\text{mol/L}$), Wortmannin, U0126, SU6656, AG490 or vehicle (DMSO 1%) for 30 min and then stimulated with PDGF-BB, IFN- γ (20 ng/mL) or thrombin (0.5 U/mL) for the indicated times. Cells were washed with ice-cold PBS and lysed in 1% (v/v) Triton X-100, 50 mmol/L HEPES, 50 mmol/L NaCl, 50 mmol/L NaF, 5 mmol/L EDTA, 10 mmol/L Na-pyrophosphate, 1 mmol/L Na-orthovanadate, 5 mmol/L phenylmethylsulfonyl fluoride (PMSF), protease inhibitor CompleteTM for 30 min. Cell lysates were centrifuged at 13,000 rpm for 10 min at 4°C and protein concentrations were determined by the Bradford method.² Equal amounts of protein (60 $\mu\text{g/lane}$ for Rb, 20 $\mu\text{g/lane}$ for all other proteins) were separated by SDS-PAGE (7.5% for Rb and STAT, 12% for MAPKs and Akt) and transferred to a polyvinylidene difluoride membrane (Bio-Rad laboratories, Austria). Equal protein loading was controlled by Coomassie Blue staining of gels. Membranes were blocked with 5% fat-free milk powder in TBS containing 1% (v/v) Tween 20 for one hr and incubated with specific antibodies at 4°C overnight. Proteins were visualized by secondary antibodies conjugated with horseradish peroxidase and ECL reagent (1 mol/L TrizmaTM Base pH 8.5, luminol 0.22 mg/mL, p-coumaric acid 0.033 mg/mL, H₂O₂ 30%) using an LAS-3000TM luminescent image analyzer (Fujifilm, Japan) and AIDATM software (raytest USA Inc., NC, USA).

Preparation of Nuclear Extracts

Cells were serum starved for 24 hrs and treated as mentioned above. Then cells were rinsed once with ice-cold PBS, harvested and centrifuged at 5,000 rpm for 5 min at 4°C. The pellet was resuspended in ice-cold hypotonic buffer (containing 10 mmol/L HEPES (pH 7.9), 10 mmol/L KCl, 0.1 mmol/L EDTA, 0.1 mmol/L EGTA, 1 mmol/L dithiothreitol (DTT), 0.5 mmol/L PMSF) and allowed to swell on ice for 15 min. NP-40 was added, samples were vortexed vigorously for 10 s and pelleted (13,000 rpm, 60 s). Nuclei were resuspended in hypertonic buffer (containing 20 mmol/L HEPES, 400 mmol/L NaCl, 1 mmol/L EDTA, 1 mmol/L EGTA, 25% (v/v) glycerol, 1 mmol/L DTT, 0.5 mmol/L PMSF), shaken for 15 min at 4°C and centrifuged (13,000 rpm for 5 min, 4°C). Supernatants were further processed for immunoblotting.

Statistical Analysis

All experiments were performed at least three times. Data are expressed as means \pm S.E.M. Statistical significance was analyzed by *t* test comparing one group with the control group. To compare two or more groups with the control group, one-way ANOVA followed by a Dunnett multiple comparison test was performed using GraphPad PRISM™ software version 4.03. (CA, USA). P values of less than 0.05 were considered significant.

References

1. Haider UG, Roos TU, Kontaridis MI, Neel BG, Sorescu D, Griendling KK, Vollmar AM, Dirsch VM. Resveratrol inhibits angiotensin II- and epidermal growth factor-mediated Akt activation: role of Gab1 and Shp2. *Mol Pharmacol.* 2005;68:41-48.
2. Bradford MM. A rapid and sensitive method for the quantitation of microgram quantities of protein utilizing the principle of protein-dye binding. *Anal Biochem.* 1976;72:248-254.

Figure I. Indirubin-3'-monoxime arrests VSMCs in G₀/G₁- and not in early S-phase. Quiescent VSMCs were stimulated with PDGF-BB for four hrs and were then synchronized in early S-phase by treatment with aphidicolin (1 μmol/L) for 15 hrs; cells treated with vehicle alone (DMSO 1%) represent the quiescent state of the cells. After washing, fresh PDGF-containing medium was added (except in vehicle control) supplemented with aphidicolin (2 μmol/L), I3MO (3 μmol/L) or vehicle. After another 10 hrs and pulse labelling with BrdU, cells were harvested, stained with a FITC-conjugated anti-BrdU antibody and 7-aminoactinomycin D and analyzed by flow cytometry. Numbers within the rectangle represent percentage of cells in the S-phase. Dot plots of one representative experiment out of three are shown.

Figure II. Indirubin-3'-monoxime has no negative impact on endothelial cell viability *in vitro*. Porcine aortic endothelial cells were incubated with DMSO (0.1%) or the indicated concentrations of I3MO for 24 hrs before their viability was analyzed according to their ability to exclude Trypan Blue. Results of one representative experiment (out of two) are depicted.

Figure III. Indirubin-3'-monoxime impairs PDGF-induced phosphorylation of the PDGF-receptor. Quiescent VSMC were treated with I3MO (3 μmol/L) for 30 min followed by a stimulation with PDGF (20 ng/mL) for the indicated periods of time. The upper panel shows a representative immunoblot depicting tyrosine phosphorylation of the receptor (overall, at Y857 and Y579/581, respectively) upon PDGF stimulation in the presence and absence of I3MO (A). The lower panels (B-D) display averaged data of the indicated tyrosine phosphorylation of the PDGFR (normalized to tubulin) obtained by densitometric analysis of four independent immunoblots. ***p<0.001; **p<0.01; *p<0.05; ns (not significant) p>0.05 (t-test)

Figure IV. Indirubin-3'-monoxime reduces translocation of phosphorylated STAT3 into the nucleus. Serum starved VSMCs were preincubated with I3MO (3 μmol/L) or vehicle (DMSO 1%) for 30 min and stimulated with PDGF-BB (20 ng/mL) for 10, 30 or 60 min. Cytosolic (A)

and nuclear (A, B) protein levels of phosphorylated STAT3^{Y705} (pSTAT3) and total STAT3 (STAT3) were determined. Images show one representative immunoblot out of three experiments.

Figure V. Indirubin-3'-monoxime diminishes long-term phosphorylation of STAT3. VSMCs were preincubated with I3MO in the indicated concentrations or vehicle (DMSO 1%) for 30 min and stimulated with PDGF-BB (20 ng/mL) for 2, 12 or 18 hrs. The expression levels of phosphorylated STAT3^{Y705} (pSTAT3) and total STAT3 (STAT3) were determined; tubulin was used as loading control. One representative immunoblot out of three experiments is shown.

Supplemental figures

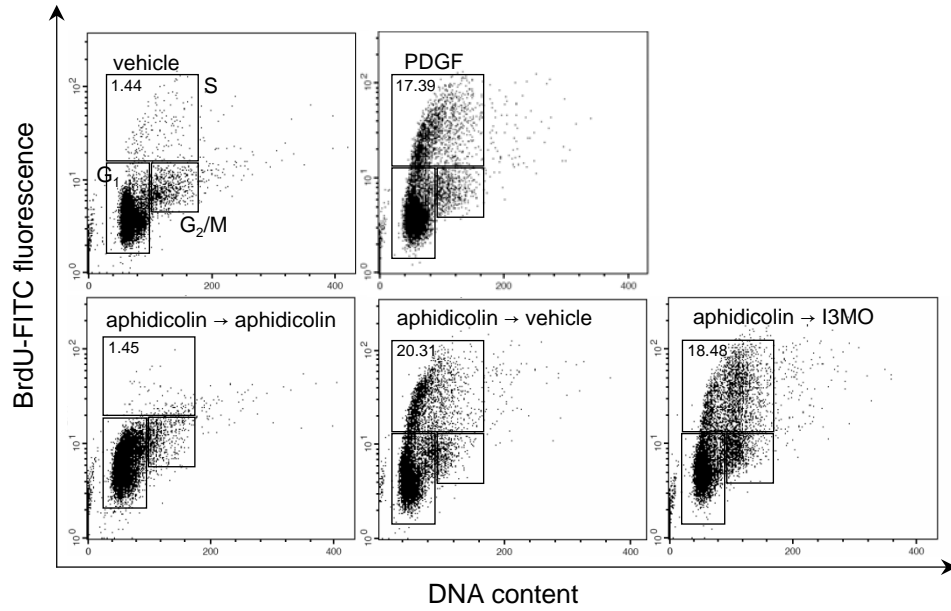


Fig. I

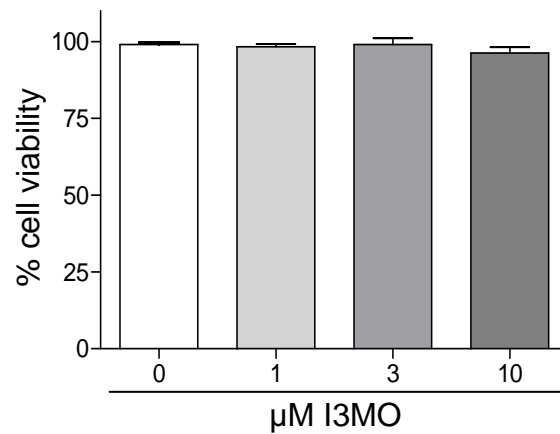


Fig. II

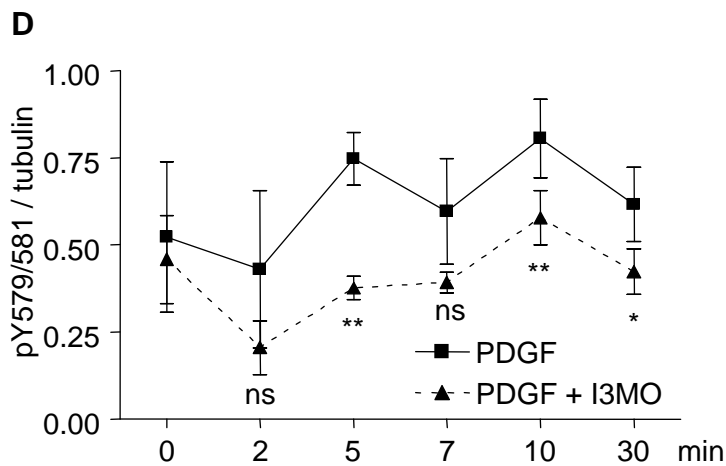
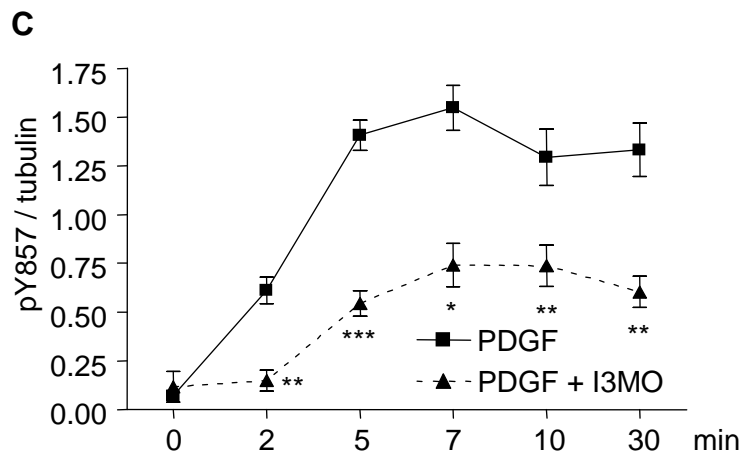
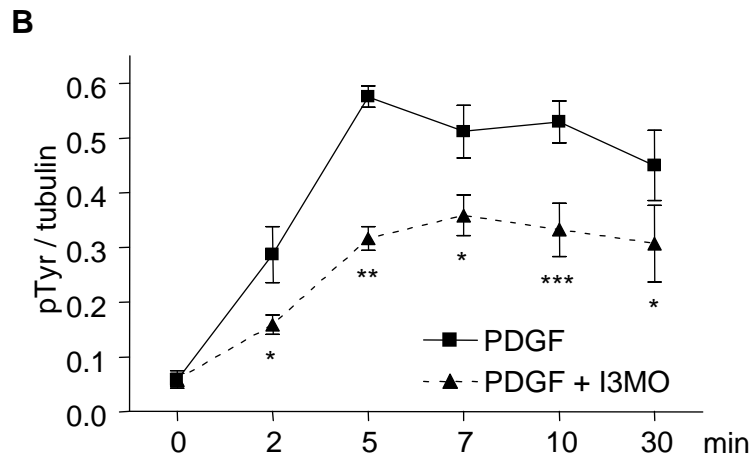
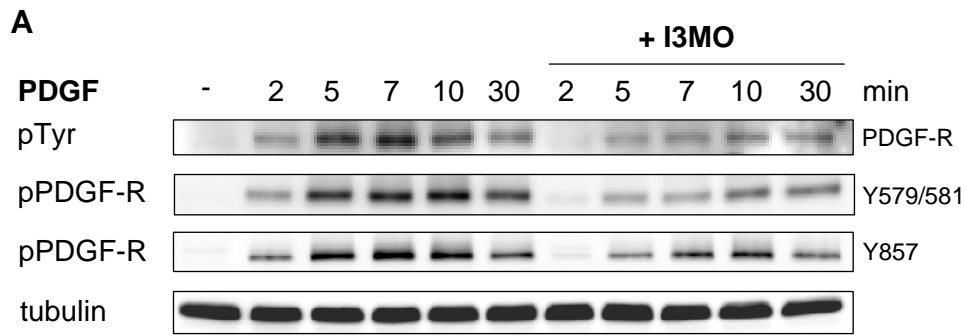


Fig. III

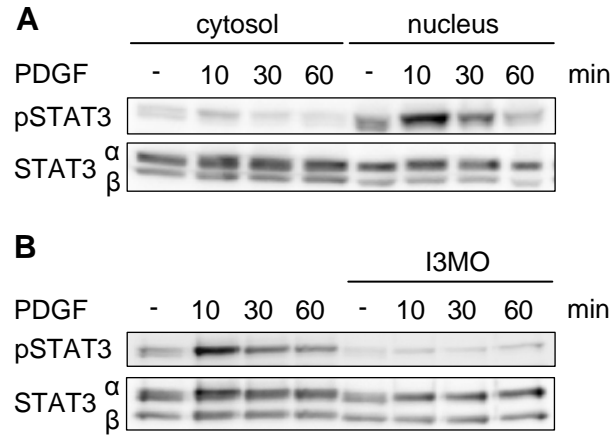


Fig. IV

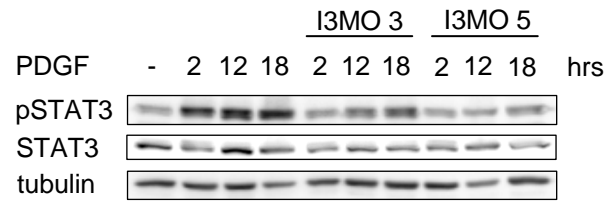


Fig. V